



# Hydrochemistry and hydrogen sulfide generating processes in the Malm aquifer, Bavarian Molasse Basin, Germany

Christina Mayrhofer · Reinhard Niessner ·  
Thomas Baumann

**Abstract** Knowledge about the hydrochemical conditions of deep groundwater is crucial for the design and operation of geothermal facilities. In this study, the hydrochemical heterogeneity of the groundwaters in the Malm aquifer, Germany, is assessed, and reasons for the extraordinarily high H<sub>2</sub>S concentrations in the central part of the Bavarian Molasse Basin are proposed. Samples were taken at 16 sites, for a total of 37 individual wells, to analyze cations, anions, gas loading and composition. The hydrochemical characteristics of the Malm groundwater in the center of the Molasse Basin are rather heterogeneous. Although the groundwater in the central basin is dominated by meteoric waters, there is a significant infiltration of saline water from higher strata. Care has to be taken in the interpretation of data from geothermal sites, as effects of chemical stimulation of the boreholes may not be fully removed before the final analyses. The distribution of H<sub>2</sub>S in the gas phase is correlated to the gas loading of the water which increases in the central basin. Temperatures, isotopic data and the sulfur mass balance indicate that H<sub>2</sub>S in the central basin is related to thermochemical sulfate reduction (south of Munich) and bacterial sulfate reduction (north of Munich).

**Keywords** Geothermal · Carbonate rocks · Germany · Hydrochemistry · Thermal conditions

Received: 20 December 2012 / Accepted: 10 October 2013  
Published online: 12 December 2013

© Springer-Verlag Berlin Heidelberg 2013

Published in the theme issue “Hydrogeology of Shallow Thermal Systems”

C. Mayrhofer · R. Niessner · T. Baumann (✉)  
Institute of Hydrochemistry,  
TUM, Munich, Germany  
e-mail: tbaumann@tum.de  
Tel.: +49-89-218078234

C. Mayrhofer  
e-mail: christina.mayrhofer@gmx.de

R. Niessner  
e-mail: reinhard.niessner@tum.de

## Background

Geothermal exploration of the Malm aquifer in the Bavarian Molasse Basin is very active with a focus on the area around Munich where nine geothermal projects are already operating successfully and a dozen new projects are in progress. The geothermal wells extend into the Malm aquifer which is located between 1,500 and 5,500 m below ground surface. Typical production rates of the geothermal wells are in the range of 30–150 L/s and the production temperatures reach up to 160 °C. There was no a priori information about the hydrochemical conditions as the geothermal wells were, and still are, the first sampling points in this area. Nevertheless, the hydrochemical composition of the Malm groundwater is as important as the hydraulic conditions, because of precipitation and corrosion issues, and safety concerns arising from the presence of significant gas concentrations; therefore a screening and monitoring program was launched with financial support from the German Federal Ministry for the Environment, Nature Conservation and Nuclear Safety. Within the scope of this study, five geothermal projects with nine wells in the central basin underwent detailed hydrochemical and isotopic analysis and gas phase characterization.

The Bavarian Molasse Basin is a sedimentary foreland basin located in South Germany (see marked area in Fig. 1). One hundred and fifty million years ago in the Late Jurassic a large sea-level rise flooded the southern region of Germany. In this marine environment, different types of carbonates were deposited. Compact and layered carbonates were formed in lagoons and flat settings, whereas reef or compacted limestones were built of reef debris. At the end of the Jurassic, the sea level fell and the carbonate sediments were partly exposed at the land surface during the Cretaceous leading to karstification. In the Tertiary, the Molasse Basin was formed as a result of the Alpine orogenesis and the eroded debris was deposited there. The western part of the Molasse Basin is dominated by terrestrial sedimentation, whereas the eastern part has a mainly marine character (Bayer. Geol. Landesamt 1996).

From the northern margin to the central basin at the edge of the Alps, the basin depth reaches up to 6,000 m. The main target for geothermal exploration in the

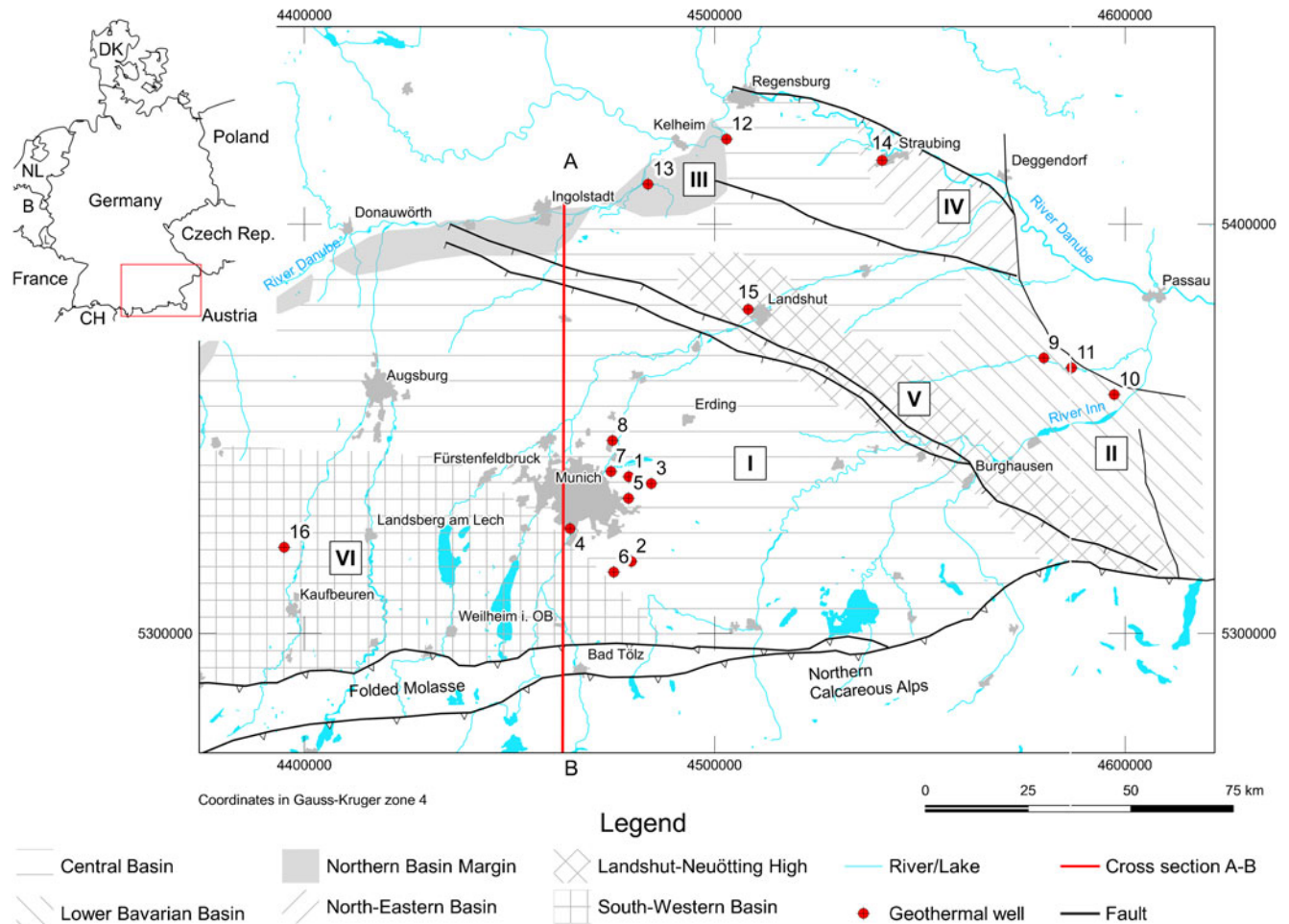


**Fig. 1** Overview of the study area (regions redrawn from Birner et al. 2011)

Bavarian Molasse Basin is the upper Malm formation. It is a carbonate-karstified deep groundwater aquifer which dips to the south and attains a vertical thickness up to 600 m in the Southern Franconian Alb and beneath the Southern Molasse sediments (Prestel et al. 1991; see schematic cross-section in Fig. 2).

The composition of the Malm thermal water in the Molasse Basin changes from the margin regions to the central basin. The groundwaters in the recharge regions at the margin of the basin are dominated by young meteoric water. It has been shown that infiltration of waters from upper formations increases with increasing aquifer depth in the western part of the Molasse Basin (Prestel et al. 1991). Here, the concentration of total dissolved solids (TDS) shows an increasing trend from north (meteoric water) to south (meteoric water with local supply of higher mineralized waters). An increase of TDS has also been postulated for the central basin. Furthermore, based on the hydrochemical characterization of the Malm groundwater close to the River Danube and in the Eastern Molasse Basin, the following hypotheses about the hydrochemical characteristics have been postulated:

- Sulfate concentrations decrease from the basin margins to the central basin (Prestel et al. 1991).
- The Malm groundwater is a mix of meteoric water and formation water seeping from the overlying sediments (Hesse and Schmidt-Thomé 1975; Prestel et al. 1991; Udluft 1975; Villinger 1977).
- Waters with the hydrochemical character of the Malm groundwater in the central basin have also been observed at the northern basin margin (Prestel et al. 1991). This process is explained as an inflow of groundwater at faults and fissures from the central part (Baumann and Quentin 1981).
- The general flow regime relevant for the study area is from the recharge areas in the northwest to the central basin near Munich and from there to the southeast (Wagner et al. 2009).

The first analyses from the geothermal wells in the central basin south of Munich in this study showed a hydrochemical composition which did not only contradict some of these hypotheses, but also revealed a high gas loading up to 0.5 L gas per L of groundwater. The main components of the gas phase are methane, carbon dioxide,

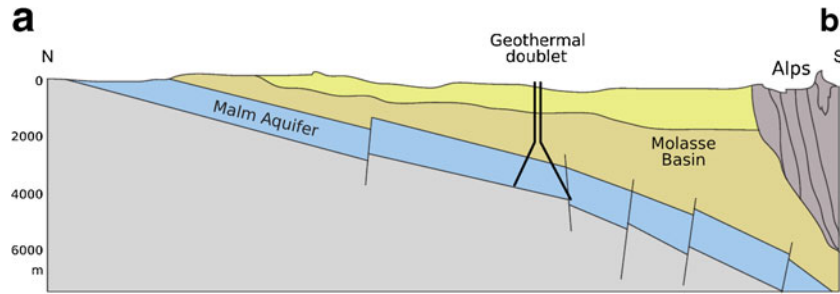


Fig. 2 Schematic cross section of the Bavarian Molasse Basin

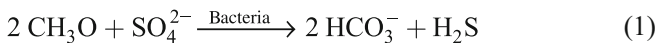
and nitrogen. The concentrations of  $\text{H}_2\text{S}$  in the gas phase reached a surprisingly high level in the percent range. Not only is  $\text{H}_2\text{S}$  a severe risk to human health but also a critical component with respect to technical safety as it causes corrosion in steel pipes, heat exchangers and other materials (Macdonald et al. 1978; Morris et al. 1980). Initially, given that  $\text{H}_2\text{S}$  concentrations in this range were considered very unlikely for groundwater, impregnation of the thermal water with sour gas from a gas reservoir was assumed to be the cause for the high concentrations of  $\text{H}_2\text{S}$  in the gas phase. Consequently, additional safety measures, like preventers, would have been required.

However, impregnation with sour gas, regardless of its origin, is only one possible mechanism leading to high concentrations of  $\text{H}_2\text{S}$  in the gas phase. The key question raised at the outset of this study was, whether the geothermal wells are in contact with a small gas reservoir containing sour gas or if the high concentrations of  $\text{H}_2\text{S}$  in the gas phase are the result of sulfate reduction in the aquifer, leading to high  $\text{H}_2\text{S}$  concentrations in the aqueous phase, followed by degassing and stripping of  $\text{H}_2\text{S}$  from the thermal water during production.

The processes which have to be considered as a source for  $\text{H}_2\text{S}$  in the Malm aquifer are thermal decomposition of organic sulfur, dissolution of pyrite, bacterial sulfate reduction (BSR), and thermochemical sulfate reduction (TSR).

During acidic stimulation of the wells, pyrite can be dissolved from the Malm limestones. As the pyrite in limestones is known to have  $\delta^{34}\text{S}$  values  $< 0$  (Clark and Fritz 1997),  $\text{H}_2\text{S}$  generated by dissolution of pyrite is characterized by depleted  $\delta^{34}\text{S}$  values in the range of  $-10$  to  $-25$  ‰ (Schulte et al. 1997). Thermal decomposition of organic sulfur compounds in kerogen or oil requires reservoir temperatures greater than  $200$  °C (Krouse et al. 1987). The temperatures in the study area are well below  $200$  °C; therefore, this explanation was not pursued.

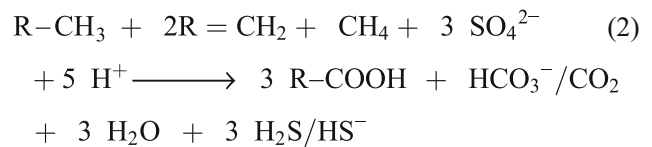
BSR can be described by a simplified net reaction (Nöth 1997):



Here  $\text{CH}_3\text{O}$  is representative of organic matter like humic substances, organic acids, hydrocarbons, or solid organic matter. Sources of dissolved sulfate can be connate waters, anhydrite dissolution, buried seawater or evaporitic brines,

decomposition of organosulfur compounds, and/or dissolution of sulfur-bearing mineral deposits. BSR is an instantaneous reaction, mass limited with respect to sulfate and organic matter, and, under typical reservoir conditions, mainly transport limited with respect to the sulfate transport to the bacteria (Berner 1980). Furthermore, bacteria can reduce sulfate only as long as the  $\text{H}_2\text{S}$  concentration is below the toxicity level for bacterial metabolism (Reis et al. 1992). BSR is a common process at lower reservoir temperatures and produces  $\text{H}_2\text{S}$  concentrations in the gas phase in the range of 3–10 %. While most sulfate-reducing bacteria prefer temperatures up to  $80$  °C (Machel 2001; Orr 1977), some hyperthermophilic sulfate-reducing bacteria even exist at temperatures up to  $110$  °C (Jørgensen et al. 1992); however, presumably with limited activity. The isotopic composition of  $\text{H}_2\text{S}$  produced by BSR is strongly dependent on the precursor sulfate and yields a wide range of  $\delta^{34}\text{S}\text{-H}_2\text{S}$  values between  $+20$  and  $-40$  ‰ (Emery and Robinson 1993). At the northern basin margin *Desulfovibrio desulfuricans* was detected in groundwaters with temperatures in the range from  $10$  to  $60$  °C (Baumann and Quentin 1981). A recent study in the central basin revealed the presence of *Desulfococcus*, *Thermodesulfuridis*, and *Desulfotomaculum*. The latter was detected even at groundwater temperatures above  $100$  °C (Alawi et al. 2011); however, the presence of both, sulfate and sulfide, at this site points to a greatly reduced activity of the bacteria.

Thermochemical reduction of sulfate (TSR) starts at temperatures in the range of  $100\text{--}140$  °C. The reaction for TSR is outlined in Eq. (2) (Goldhaber and Kaplan 1974; Machel 1987; Machel et al. 1995; Nöth 1997; Orr 1977):

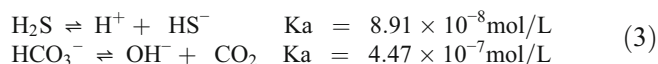


where R- stands for high molecular weight alkanes, alkenes, and methane. TSR reaction rates are controlled by the temperature, the concentration and type of reactive organic material (gaseous, oil, solid), and the concentration of sulfate. As Liu et al. (2013) point out based on their previous work, minimum temperatures are



higher (> 140 °C) for TSR by gas compared to > 110 °C for TSR by oil. High H<sub>2</sub>S concentrations are often associated with methane-rich gases (Orr 1982). The sources for sulfate are the same as for BSR. Reactive organic material can be sedimentary organic matter, dissolved organic carbon, crude oil, microbial methane, thermogenic gas and/or gas condensate. Furthermore, the composition of the total gases, catalysts, sulfate availability and migration/diffusion rates of the major reactants play a role for the rate of TSR (Machel 2001). As the porosity of the reservoir indirectly controls the TSR rates dolomite reservoirs (e.g. Sichuan and Ordos Basin, China) usually show higher H<sub>2</sub>S concentrations than limestone reservoirs because of a higher matrix porosity in dolomites. In addition, Mg<sup>2+</sup> can catalyze TSR (Zhu et al. 2007a).

The products of TSR according to Eq. (2) are H<sub>2</sub>O, H<sub>2</sub>S/HS<sup>-</sup>, HCO<sub>3</sub><sup>-</sup>/CO<sub>2</sub>, and organic sulfur compounds. The relative proportions of H<sub>2</sub>S/HS<sup>-</sup> and HCO<sub>3</sub><sup>-</sup>/CO<sub>2</sub> highly depend on pH. The dissociation reactions and dissociation constants (K<sub>a</sub>) at 25 °C are given in Eq. (3) (Perrin 1982):



TSR produces H<sub>2</sub>S concentrations in the gas phase up to 90 %. Data from deep buried carbonate reservoirs in the Alberta Basin in Canada show a δ<sup>34</sup>S–H<sub>2</sub>S of 20.1±1.5 ‰, whereas the corresponding anhydrite showed a range of 22.7–33 ‰ (Emery and Robinson 1993). In laboratory experiments the observed kinetic isotope fractionation by TSR was close to zero; consequently, the isotopic composition of produced H<sub>2</sub>S is similar or a few per mil lighter than precursor sulfate (Krouse et al. 1988; Orr 1977). Orr (1974) indicated that as a result of TSR the H<sub>2</sub>S content increases with increasing temperature, after examining isotopic measurements of Big Horn paleozoic oils in Wyoming, USA. Furthermore, the sulfur isotopic composition of reduced organic and inorganic sulfur changed towards that of reservoir sulfate. In other field studies, higher fractionation factors were observed. Zhu et al. (2007b) determined in the Weiyuan Gas Field, Sichuan Basin, China typical isotope fractionation values for TSR of 8–12 ‰, which are comparable to the fractionation values in the Alberta Basin. Wynn et al. (2010) recorded isotopic fractionation values up to 53 ‰ in Cerna Valley, Romania, which are much higher than expected for TSR. This was attributed to incomplete TSR a unique hydrogeologic setting, and a contribution of BSR along the flow path.

Finally, kinetic isotope fractionation, although variable, yields ratios of –25 to –50 ‰ (Goldhaber and Kaplan 1974); however, the rates for isotopic exchange between dissolved sulfide and sulfate is slow at temperatures below 200 °C (Emery and Robinson 1993). Despite all differences, both the isotopic ratio and isotope

fractionation depend on the precursor sulfate and change along the reaction path in a closed system; therefore, an interpretation based on isotopic data alone carries some ambiguity.

This study connects hydrochemical data, gas analyses and isotope analyses to bring new insights in the generation processes of H<sub>2</sub>S in the Malm aquifer. It also introduces new data on the hydrochemical characteristics, especially for the central part of the Molasse Basin where no groundwater wells had been previously available, to reduce the uncertainty for geothermal exploration.

## Materials and methods

### Water sampling

Samples were taken at the well head. When the temperatures were above 98 °C, the samples were taken using a cooler, or after the heat exchanger if available. The water temperature, pH, redox potential (E<sub>h</sub>), and electrical conductivity (EC) were measured with pH 330 (WTW), Redox SenTix ORP chain (Ag/AgCl 3.5 mmol KCl), and LF 92 (WTW) on-site. Chloride, iodide, and bromide were measured using ion chromatography with EC detector (IC 25, IonPac AS9-HC column, Dionex). Sodium and potassium were measured using atomic emission spectrometry (ELEX 6361, Eppendorf). Calcium was titrated with EDTA, and magnesium was measured using flame atomic absorption spectrometry (AAS 3300, Perkin Elmer). Dissolved sulfides in water (S<sup>2-</sup>, HS<sup>-</sup> and H<sub>2</sub>S) were precipitated on-site with 10 mL zinc acetate (2 %). The concentration of the precipitated zinc sulfide was measured with the methylene blue colorimetric method (Deutsches Institut für Normung 1995) using a spectrophotometer (Double Beam UV-190, Shimadzu). Analytical errors were determined using six samples taken at site 4 collected within 20 min. For cations and anions the analytical error is between 2 and 11 %.

### Gas sampling

Gas samples were collected with two different methods. For the first method, a constant flow of thermal water was established through an on site gas stripping column made of polypropylene. The pressure inside the stripping column was established at 10 hPa above atmospheric pressure. The gas loading was calculated by dividing the volume of gas inside the semi-transparent column by the measured volume of thermal water which passed through the column. The separated gas phase was transferred into two glass gas sampling tubes (Witeg). Samples for analysis were taken out of the gas sampling tubes.

Additionally, and at lower gas loadings, the thermal water was transferred into 0.4-L double-ended stainless steel containers at a pressure of about 0.4 MPa. Here, the thermal water was first flushed through the container, then the outlet valve was closed first, followed by closing the inlet valve. For analysis, this container was connected to an evacuated glass bottle. The pressure after connecting the two containers

was recorded to calculate the gas loading. Samples for analyses were taken out of this glass bottle.

A full analysis of the gas phase was performed at five sites in the study area. The gas analysis was performed by IGU Dr. Salvamoser, Wörthsee, Germany, using gas chromatography with a thermal conductivity detector ( $N_2$ ,  $O_2$ ,  $CO_2$ ) and a flame ionization detector ( $CH_4$ ,  $C_2H_4$ ,  $C_2H_6$ ,  $C_3H_8$ ,  $C_4H_{10}$ ). As interactions of  $H_2S$  with the stainless steel container are very likely, no  $H_2S$  was determined for the samples from the stainless steel containers. Partial pressures were calculated using PHREEQC (Parkhurst and Appelo 1999) based on the full gas analyses.

For the quantification of  $H_2S$ , the gas sampling tubes were flushed with nitrogen ( $\geq 99.9\%$   $N_2$ ) and passed into three gas washing bottles (NS 45/40, Schott/Duran), which were filled with 60 mL zinc acetate (2 %) each. The concentration of sulfides was measured as described in the preceding.

The error of the relative composition of the gases with GC is on the order of 2 % and below 15 % for the determination of  $H_2S$ . The variation in gas volume was below 15 % for the on-site stripping column and less than 10 % for the analyses out of the stainless steel containers.

### Stable isotope measurements

Stable isotope measurements were performed by IGU Dr. Salvamoser, Wörthsee, Germany, at the five sites with complete gas analyses. For measuring  $^{34}S$  in sulfate, barium chloride was added to the water samples to precipitate dissolved sulfate as barium sulfate. Barium sulfate was then decomposed at high temperature to form  $SO_2$  for isotope analysis in a mass spectrometer (Bailey and Smith 1972). To determine  $^{34}S$  in sulfides, the water samples were prepared with zinc acetate immediately after sampling. The dissolved hydrogen sulfide was precipitated as  $ZnS$ . For analysis, the samples were acidified to produce  $H_2S$ , which was transferred into a  $AgNO_3$  solution to form  $Ag_2S$ , which later was oxidized at high temperatures to form  $SO_2$  for mass spectrometry analysis.  $^{18}O$  in water was determined with mass spectrometry (Epstein and Mayeda 1953). To measure  $^2H$ , the water sample was reduced in a uranium furnace at 800 °C (Coleman et al. 1982; Friedman 1953) and measured using a mass spectrometer. Results of the isotopic analyses are given relative to the Diablo Canyon Iron Meteorite scale (CDT,  $^{34}S$ ) and the Vienna Standard Mean Ocean Water (V-SMOW,  $^{18}O$  and  $^2H$ ). Analytical errors provided by the laboratory were below 5 % of the given values.

## Results and discussion

### General hydrochemical characteristics

The data presented in this study include 429 groundwater samples obtained at 37 wells, with 1–70 samples per well, and taken over a time period of 7 years. An overview of the hydrochemical characteristics is given in Table 1. The

classification into regions follows the idea of Birner et al. (2011) who divided the Bavarian Molasse Basin into six different hydrochemical provinces: the central basin (region I, sites 1–8), the Lower Bavarian Basin, (II; sites 9–11), the northern basin margin (III, sites 12–13), north-eastern basin (IV, site 14), the Landshut-Neuötting High (V, site 15) and the south-western basin (VI, site 16). For each region the median value and the interquartile range (IQR; 50 % of the data around the median falls within these values) are given. Not all of the regions have an equal number of wells and samples. Therefore, an unconditional statistical evaluation would be biased. In this study, the data of region I mainly reflect the spatial heterogeneity, while data from region VI nicely show the temporal variability of the hydrochemical conditions at one single well.

Samples taken during the initial pumping tests of freshly installed geothermal wells turned out to be heavily influenced by the drilling process and acidic stimulation. These samples are characterized by a pH-value below the average and an increase of the concentrations of calcium, magnesium and chloride. In this study, data affected by stimulation are not included in Table 1 or any other evaluation except Fig. 3. However, it is noted that some of these data, especially for those wells which are used as reinjection wells later on, are the only data available.

The temporal development of the hydrochemical conditions is shown in Fig. 3 for site 4. From the first pumping test of the well (a) to the second test (b) to the long-term equilibrium after 6 years of operation there is a decrease in the concentrations of calcium and magnesium by almost two orders of magnitude. The concentrations of chloride decrease by a factor of 10 and the concentrations of sulfate decrease by a factor of 5. The concentrations of bicarbonate are almost constant over the complete history of this well. This effect can be explained by the chemical stimulation of the well. After reaching the final depth, and an initial lift test to remove the drilling mud, HCl was injected into the well to remove traces of the drilling mud and to open the fractures. It dissolved the carbonate rock causing an increase in the concentrations of calcium, magnesium, and  $CO_2$ . At site 4, an equilibrium was reached with a standard deviation of less than 3 % only after 2 years of full operation.

The reservoir temperatures are dominated by the geothermal gradient and the flow regime in the aquifer. It has to be pointed out that most of the temperatures measured in this study were recorded at the well head. Due to significant heat loss in the well, especially during the initial pumping tests when the area surrounding of the borehole is still at ambient temperatures (Tilley and Baumann 2012), the reservoir temperatures are expected to be up to 10–15 °C higher.

In the central basin and in the south-western basin, reservoir temperatures of 90 to 140 °C are expected with increasing temperatures to the south. At the Lower Bavarian Basin and the Landshut-Neuötting High the temperatures are in a range of 50–70 °C. Reservoir temperatures of 20–30 °C

**Table 1** Hydrochemical characteristics in the different regions: median and (interquartile range)

Wells Samples	Unit	Central basin I	Lower Bavarian basin II	Northern margin III	North-eastern basin IV	Landshut-Neubüting High V	South-western basin VI
pH		20	7	7	1	1	1
EC	$\mu\text{S}/\text{cm}$	199	71	79	9	1	70
Eh (Ag/AgCl)	mV	7 (6.4–7.5)	7.4 (7.2–7.5)	7.3 (7.2–7.4)	7.4 (7.3–7.4)	6.3	6.8 (6.7–6.9)
Na <sup>+</sup>	mg/L	1,500 (830–3,100)	1,600 (1,400–1,800)	720 (710–800)	1,900 (1,900–1,900)	980	8,100 (8,000–8,200)
K <sup>+</sup>	mg/L	-330 (-360–-250)	-280 (-310–-250)	-310 (-390–-290)	-210 (-350–-130)		-220 (-280–-210)
Ca <sup>2+</sup>	mg/L	130 (120–140)	310 (290–400)	80 (71–85)	360 (340–370)	120	1,700 (1,700–1,800)
Mg <sup>2+</sup>	mg/L	18 (16–32)	17 (14–23)	8.2 (6.4–9.4)	14 (11–20)	15	50 (49–55)
Cl <sup>-</sup>	mg/L	47 (35–410)	19 (7.3–23)	51 (47–57)	32 (31–34)	41	79 (77–82)
SO <sub>4</sub> <sup>2-</sup>	mg/L	14 (12–58)	4 (1.8–5)	20 (20–23)	7.6 (7.4–7.8)	9.2	22 (21–23)
HCO <sub>3</sub> <sup>-</sup>	mg/L	270 (120–900)	170 (160–220)	46 (42–53)	400 (390–410)	80	1,700 (1,600–1,700)
S(-II) ges.	mg/L	8.4 (3.3–16)	4.1 (2–7.8)	1.8 (1.1–2.5)	4.2 (3.2–7)	2.2	850 (800–900)
HS <sup>-</sup>	mg/L	280 (190–330)	610 (600–710)	390 (380–430)			1,200 (1,100–1,200)
H <sub>2</sub> S	mg/L	4 (1.3–6)	1.7 (0.55–2.6)	4.4 (3.7–5)			0.92 (0.38–1.3)
	mg/L	1.5 (1.1–2.2)	0.99 (0.35–1.5)	3 (2.5–3.3)			0.36 (0.21–0.47)
	mg/L	2.2 (0.87–5.1)	0.45 (0.094–1.1)	1.6 (1.3–1.9)			0.54 (0.22–0.75)

are characteristic at the northern basin margin and at the north-eastern basin margin.

The pH values of the groundwater in the central basin are around 7.0 (IQR 6.4–7.5). Lower pH values were measured in the south-western basin (6.8) and higher pH values were measured in the Lower Bavarian Basin, northern basin margin and north-eastern basin (7.3/7.4). IQRs for all regions except the central part are on the order of 0.2 pH units. The EC values in the central basin show a median of 1,500  $\mu\text{S}/\text{cm}$  which is comparable to the north-eastern basin and the Lower Bavarian Basin. The IQR of 830–3,100 indicates a large spatial variation. Groundwater at the northern margin shows significantly lower EC. Site 16 in the south-western basin shows an EC value of 8,100  $\mu\text{S}/\text{cm}$ , suggesting an influence of saline waters. The decreasing redox potential towards the central basin has been postulated and is consistent with hypotheses of Prestel et al. (1991). Groundwaters with low EC are generally dominated by calcium, magnesium and bicarbonate (Ca–Mg–HCO<sub>3</sub>-type). This composition reflects the limestones and dolomites forming the Malm aquifer. Increasing EC is caused by an increase of the concentrations of sodium, chloride, and sulfate. However, only chloride reaches relative concentrations above 20 %, thus characterizing these waters as Ca–Mg–Cl–HCO<sub>3</sub>-type. This indicates the infiltration of highly mineralized waters from higher strata as suggested by Lemcke (1976) and reflects a downward oriented flow in the lower Tertiary sediments (Andres and Frisch 1981).

The hydrochemical characteristics of the groundwater in the different regions are summarized in a Piper diagram in Fig. 4. The groundwater type shows little variation within most parts of the study area, indicating homogeneous lithostratigraphic groundwater flow conditions. As most of these wells have been in operation at constant pumping rates

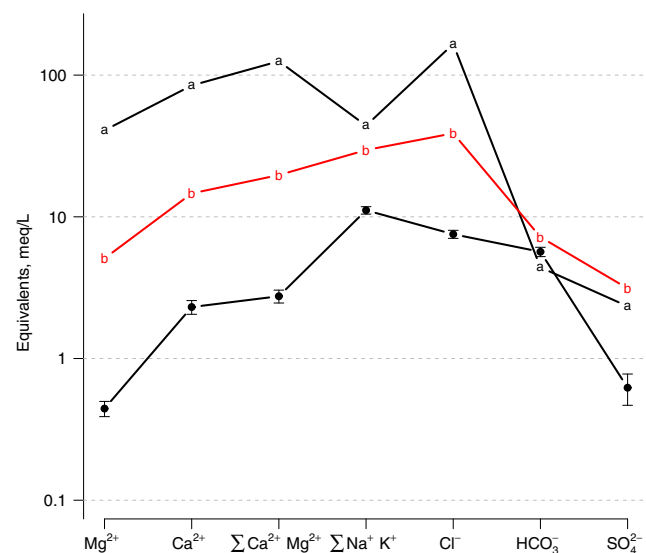


**Fig. 3** Schoeller diagram for the well at site 4. Lines *a* and *b* represent samples collected during the first and second pumping test, respectively. The *other line* shows the mean and standard deviation at equilibrium conditions obtained within 2 years of operation

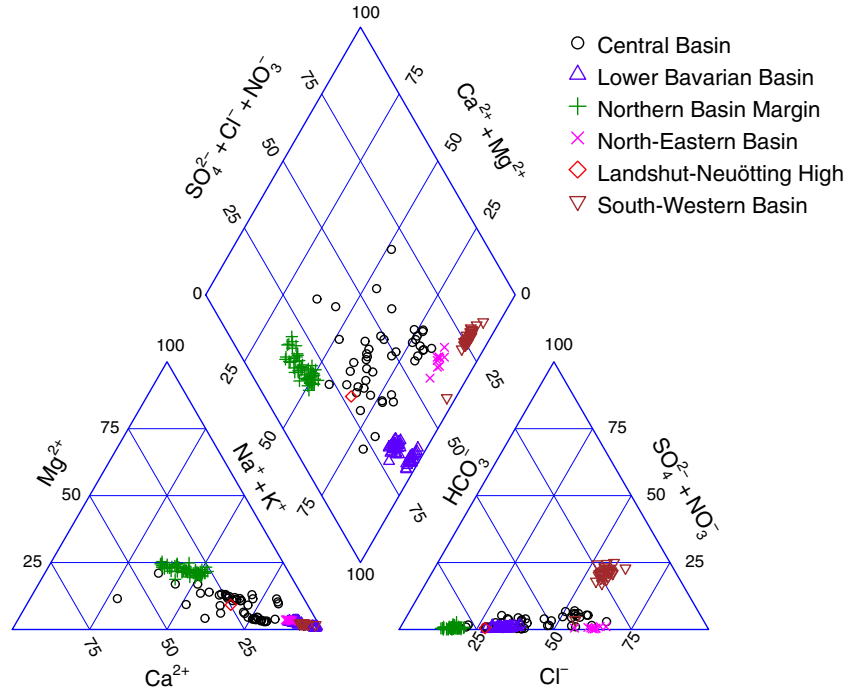


Fig. 4 Piper diagram of all tested wells in the Malm aquifer

for more than 20 years, an equilibrium between the different sources contributing to the well has been established.

Waters from the Lower Bavarian Basin are characterized by higher sodium and potassium concentrations originating from the exchange of calcium and magnesium with sodium at clay mineral exchange sites in the overlying Tertiary sediments (Na-HCO<sub>3</sub>-Cl type) as numerous analyses from the Tertiary aquifers in this area show. Samples from the northern basin margin show two different hydrochemical types. Samples from wells 12a, 12c, 13a, 13b, 13d, 13e and 13g show related characteristics to wells 9, 10 and 11 in the

Lower Bavarian Basin and can be classified as Na-HCO<sub>3</sub>-Cl waters. The other hydrochemical group (well 12b, 13c and 13f) is characterized by lower potassium and chloride concentrations as well as higher bicarbonate concentrations. These wells characterize a Ca-Na-Mg-HCO<sub>3</sub> water type. The general water type of site 14 in the north-eastern basin is Na-Cl-HCO<sub>3</sub>/Na-Ca-Mg-HCO<sub>3</sub>. Waters from well 15 at the Landshut-Neuötting High show a Na-Ca-HCO<sub>3</sub>-Cl type. Site 16 in the south-western basin shows an extraordinary composition with a TDS of 5.8 g/L and high concentrations of natural gas and hydrocarbons. This is unusual for Malm groundwater and cannot be explained with an interaction with the limestone alone. As this well is close to an oil and gas field, the groundwater is possibly affected by oilfield waters.

The situation in central basin, however, is more complicated. A high spatial heterogeneity was observed. In general, groundwaters of Ca-Mg-HCO<sub>3</sub> type dominate. Infiltrating waters are richer in sodium and chloride (Carlé 1975; Lemcke 1988) and might change the groundwater type. Lower sodium, chloride and sulfate concentrations were observed north of Munich which suggests less infiltration compared to the deeper groundwater south and south-southeast of Munich.

The main constituents of the Malm aquifer are limestone and dolomite, which are reflected in the calcium-to-magnesium ratio. The Ca/Mg ratios in the groundwater in the central Malm aquifer are in the range of 0.8 to 8.5 with a median of 3.8. Ca/Mg > 2.2 represents water in contact with limestone, while Ca/Mg < 2.2 indicates water in contact with dolomites (Langmuir 1971). Lower ratios are observed at the northern basin margin and high ratios in the central basin and in the Lower Bavarian Basin.

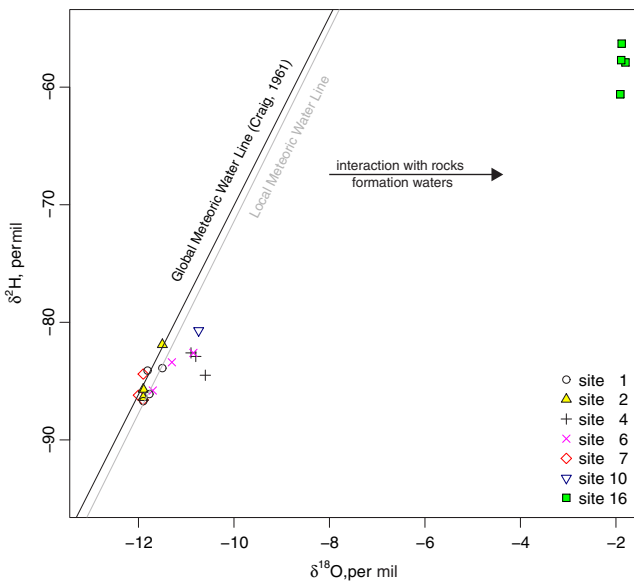


Fig. 5  $\delta^2\text{H}/\delta^{18}\text{O}$  ratio at five sites in the central basin (base graph from Domenico and Schwartz 1998)



**Table 2** Gas composition at eight wells in the central basin

Well	Gas volume NmL/L	CO <sub>2</sub> Vol %	N <sub>2</sub> Vol %	O <sub>2</sub> /Ar Vol %	CH <sub>4</sub> Vol %	H <sub>2</sub> S Vol %	Remarks
1a	100.8	5.9	50.4	0.3	43.0	0.3	1st pumping test
2a	49.1	60.4	11.7	NM	19.2	8.7	1st pumping test
2a	65.2	55.9	24.4	0.6	14.2	4.9	2nd pumping test
2a	24.1	62.7	12.5	0.5	24.3	NM	2nd pumping test
4	330.0	38.9	4.6	0.2	54.5	0.6	In operation
6a	107.8	31.7	26.8	0.8	40.0	0.7	1st pumping test
6a	59.2	55.9	30.8	0.6	6.7	6.1	2nd pumping test
6b	16.9	19.9	72.6	0.3	7.3	NM	After stimulation
6c	57.7	89.5	5.4	0.5	3.3	1.3	After stimulation
7a	47.8	36.7	25.6	0.6	35.2	2.1	Pumping test
7b	24.4	45.0	30.1	0.5	24.4	NM	Pumping test

NM not measured

**Isotopic signature of the Malm groundwater**

Figure 5 shows the ratio of  $\delta^2\text{H}$  to  $\delta^{18}\text{O}$ , and the global (GWML; Craig 1961) and local meteoric water line (LMWL). The LMWL is slightly shifted to lower  $\delta^2\text{H}$  values reflecting both, the latitude and continental effects. Most of the groundwaters are situated around the LMWL for Middle Europe, indicating meteoric waters as primary source. In the central basin the values of  $\delta^{18}\text{O}$  are between  $-10.4$  and  $-11.9$  ‰ and the values of  $\delta^2\text{H}$  are from  $-79.9$  to  $-86.7$  ‰. The  $\delta^{18}\text{O}$  and  $\delta^2\text{H}$  values reflect the isotopic fractionation during evaporation and precipitation. Low values indicate low ambient temperatures and are usually assigned to the last ice age (Pleistocene). For instance the groundwater in the Styrian basin (Austria) shows  $\delta^2\text{H}$  values of  $< -70$  ‰ and was assigned to generation temperatures of  $4.6$  °C (Goldbrunner 1997). Another study puts temperatures of  $5$  °C to waters with isotopic signatures of  $\delta^2\text{H}$  between  $-95$  and  $-75$  ‰ and  $\delta^{18}\text{O}$  between  $-12.8$  and  $-10.6$  ‰ (Stichler et al. 1987). Consequently, the Malm groundwater can be assigned to the same climatic conditions and be considered

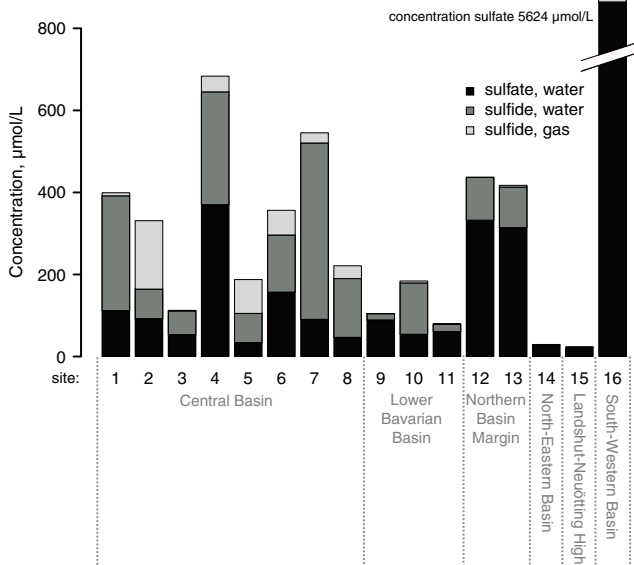


**Fig. 6** Sulfur concentrations and speciation in the study area

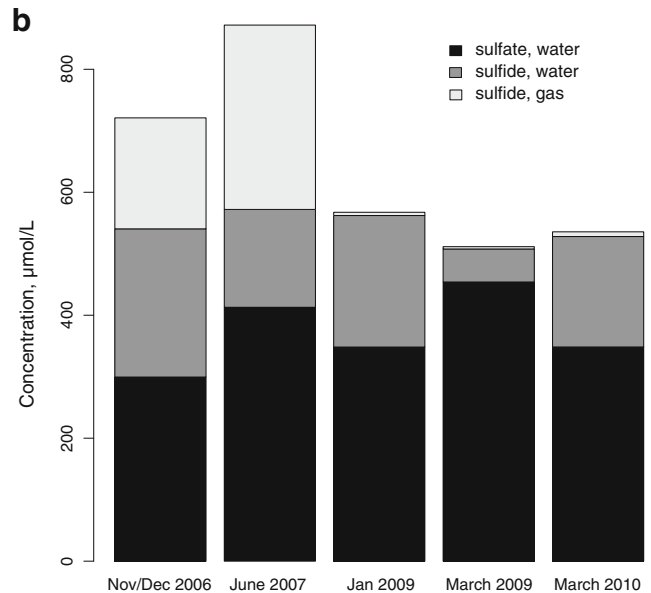
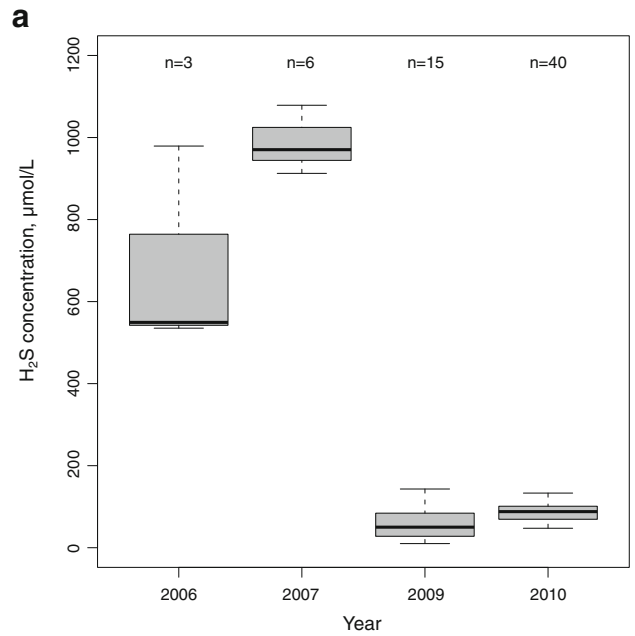


**Fig. 7** a Boxplot of the H<sub>2</sub>S concentrations at site 4 from 2006 to 2010 and b the sulfur concentrations and speciation at site 4



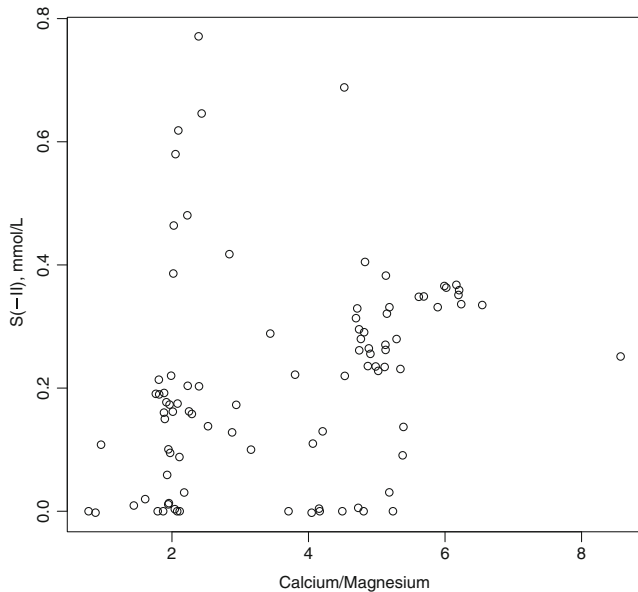


**Fig. 8** Total sulfide concentrations as a function of the calcium/magnesium ratio

of Pleistocene Age with a minimum age of 8,000–12,000 years.

The isotopic signature of the groundwater at site 16 clearly deviates from the LMWL with  $\delta^{18}\text{O}$  of values of  $-1.9\text{‰}$  and  $\delta^2\text{H}$  of  $-58\text{‰}$ , indicating an influence of formation waters. Together with the high gas loading, the hydrochemical characteristics and high concentrations of hydrocarbons, a connection to an oil reservoir seems likely, although the nearest oil field is at 20 km distance and located in the Tertiary sediments. In the Munich area, site 4 shows slightly higher  $\delta^{18}\text{O}$  values than the rest ( $10.9\text{‰}$ ),

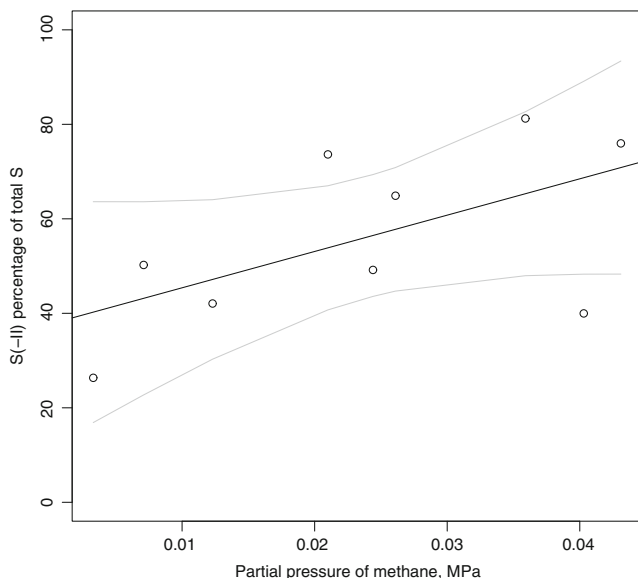


**Fig. 9** Percentage of sulfides of total sulfur in gas and water as a function of the methane partial pressure with regression line and confidence intervals

supporting the assumption of an influence of higher mineralized waters from the superstructure.

### Gas composition in the Malm aquifer

The results of the screening of the gas composition at eight geothermal wells at five sites in the central basin are given in Table 2. Here, gas samples were taken after acidic stimulation, during initial and long-term pumping tests, and during operation.

The total gas volume per liter of thermal water in the central basin is in the range of 4.0–900 NmL/L with a median of 70 NmL/L and an IQR from 41 to 113 NmL/L. Under reservoir conditions, all gases are dissolved; however, with partial pressures up to 1.5 MPa in the central basin, degassing during production is likely to occur. At low gas concentrations,  $\text{CO}_2$  dominates the gas phase. The concentration of  $\text{CO}_2$  matches the carbonate equilibrium; excess  $\text{CO}_2$  was detected only after acidic stimulation. With increasing gas concentrations, the fraction of methane increases, while the fraction of  $\text{N}_2$  is rather constant with an IQR of 11–27 vol-%. There is a general trend to lower concentrations of  $\text{H}_2\text{S}$  with increasing gas loading. This suggests a mass limited process as source of  $\text{H}_2\text{S}$  in the gas phase which is consistent with the hypotheses of  $\text{H}_2\text{S}$  being stripped from the thermal water during production. On the other hand, this contradicts an impregnation with sour gas from a gas reservoir, which would yield of a constant concentration of  $\text{H}_2\text{S}$  in the gas phase.

The average concentrations of all sulfur species in gas phase and water are given in Fig. 6 for each of the 16 geothermal sites in the study area. With pH values between 6.8 and 7.8 the ratio between  $\text{HS}^-$  and  $\text{H}_2\text{S}$  is between 67:33 and 95:5 at 120 °C. However, only  $\text{H}_2\text{S}$  will be stripped from the thermal water, thus causing the sulfur species to reequilibrate and eventually leading to a complete stripping of S(-II) from the thermal water.

The highest sulfur concentrations were measured in the south-western basin at site 16, where sulfate dominates with 5.6 mmol/L. Waters from the Lower Bavarian Basin, the north-eastern basin and the Landshut-Neuötting High generally show lower sulfur concentrations. Total  $\text{H}_2\text{S}$  concentrations are highest in the central basin, followed by the northern basin margin, an area where several springs contain dissolved  $\text{H}_2\text{S}$  and which is known for its Roman spas. The measured total  $\text{H}_2\text{S}$  concentrations and especially the  $\text{H}_2\text{S}$  concentrations in the gas phase show a high variance. The highest concentrations of  $\text{H}_2\text{S}$  in the gas phase were observed in central basin with up to 170  $\mu\text{mol/L}$  or 8.7 vol %. Outside the central basin,  $\text{H}_2\text{S}$  concentrations in the gas phase are low to negligible, reflecting the lower temperatures and low total gas concentrations.

An assessment of the short and long-term variations of the  $\text{H}_2\text{S}$  concentrations in the gas phase was performed at site 4 in 2009 and 2010. This site has been in full production at an average production rate of 32 L/s since 2005. There was a decrease of the  $\text{H}_2\text{S}$  concentrations from 885  $\mu\text{mol/L}$  in 2006/2007, to an average of 80  $\mu\text{mol/L}$  in 2010 (see Fig. 7a). During this time, the gas concentrations remained in the same

range at an average value of  $190 \pm 80$  NmL/L. Also the sulfur speciation in water shows little variability. The  $\text{H}_2\text{S}$  concentration is above average in 2006/2007 (see Fig. 7b).

While the monitoring in 2009 indicates that the  $\text{H}_2\text{S}$  concentrations might depend on the flow rate, the 2010 monitoring campaign did not support this assumption. Rather it seems that the  $\text{H}_2\text{S}$  concentration at this site is mainly controlled by natural short-term variations in the gas loading.

The effect of the geological facies on the  $\text{H}_2\text{S}$  concentration is shown in Fig. 8, where the calcium/magnesium ratio is plotted against the  $\text{H}_2\text{S}$  concentration, if both values were measured. Although magnesium catalyzes TSR and a higher porosity in dolomites might support the production of  $\text{H}_2\text{S}$  by TSR (Zhu et al. 2007a), there is no clear trend in the data for the central basin.

Figure 9 shows the relation between the ratio of S(-II) to total sulfur and the partial pressure of methane in MPa. With increasing partial pressure of methane there is an increasing fraction of sulfides. This supports TSR as outlined in Eq. (2), but also indicates that a thermodynamic equilibrium has not been reached. This might indicate that infiltration is faster than TSR under the given conditions.

The values of  $\delta^{34}\text{S}-\text{H}_2\text{S}$  in the central basin are in a range of +3.2 to +9.7 ‰ and the values of  $\delta^{34}\text{S}-\text{SO}_4^{2-}$  range from +8.5 to +20.8 ‰. Isotopic fractionation values for  $\delta^{34}\text{S}-\text{SO}_4^{2-} - \delta^{34}\text{S}-\text{H}_2\text{S}$  were calculated and are between 3.4 and 17.6 ‰. Thus, both processes, TSR and BSR, are possible and the temperature regime seems to control the sulfate reduction process. Production of  $\text{H}_2\text{S}$  by dissolution of pyrite during acidic stimulation can be ruled out because the values of  $\delta^{34}\text{S}-\text{H}_2\text{S}$  from sedimentary pyrite in limestone are expected to be  $< 0$ .

## Conclusions

The hydrochemical conditions in the Malm aquifer in the Bavarian Molasse Basin can be mainly characterized as the result of meteoric waters interacting with the carbonates that make up the Malm aquifer. The hydrochemical analyses, although showing a great degree of variation, generally mirror the lithostratigraphic setting. This implies slow groundwater movement in the Malm aquifer in order to reach equilibrium conditions. In the central basin, mixing with groundwater from higher strata leads to an increase of the concentrations of sodium and chloride. Stable isotopic analyses for the central basin suggest a traveltime from the recharge areas to the central basin around Munich of at least about 10,000 years. There are two exceptions, one located in the central basin south of Munich and one in the western part of the basin. The site south of Munich is influenced by waters with higher mineralization, infiltrating from the superstructure. The site in the south-western basin is most likely influenced by oil field waters. It has to be understood that the hydrochemistry of a geothermal well cannot be determined from the first pumping tests if acidic stimulation has previously taken place. Data also suggests that it might take up to 2 years of full operation to establish a

hydrochemical equilibrium. Gas loadings seem to decrease during operation, but monitoring data are not yet sufficient to predict short-term and medium-term variation.

The highest sulfide concentrations in water and  $\text{H}_2\text{S}$  concentrations in the gas phase were measured in the central basin. Prestel et al. (1991) assumed a trend of decreasing sulfate concentrations to the central basin with increasing sulfide concentrations. This hypothesis has been generally supported by the data obtained in this study. However, infiltrating waters may lead to a coexistence of sulfate and sulfide. The fractionation values for  $\delta^{34}\text{S}$  suggest incomplete reduction of sulfate to sulfide in the southern central part, because the isotopic signatures of  $\delta^{34}\text{S}-\text{H}_2\text{S}$  and  $\delta^{34}\text{S}-\text{SO}_4^{2-}$  differ. TSR and BSR occur in two mutually exclusive thermal regimes (Machel 2001; Nöth 1997; Orr 1977). Based on the results of this study, TSR is expected to be the  $\text{H}_2\text{S}$  generating process in the southern part of the Bavarian Molasse Basin, because the reservoir temperatures exceed the possible range for BSR of almost 110 °C. TSR is also known for the generation of higher  $\text{H}_2\text{S}$  concentrations compared to BSR. Indications for TSR in the central basin can also be detected in the relation between the methane partial pressure and the  $\text{H}_2\text{S}$  concentrations. For low temperature settings like the Lower Bavarian Basin, northern basin margin, north-eastern basin, Landshut-Neuötting High and the south-western basin BSR is supposed to be the  $\text{H}_2\text{S}$  producing mechanism. This is in agreement with results at the northern basin margin, where reduction of sulfate to sulfide by bacteria was confirmed by the analysis of pyrite-marcasite-geodes (Baumann and Quentin 1981). Production of  $\text{H}_2\text{S}$  by degradation of organic sulfur compounds to sulfides is not likely in the Malm aquifer, because the required temperatures of 200–300 °C are not reached even in the deepest parts of the Malm aquifer close to the Alps. Finally, the results of this study rule out the impregnation of the waters in the Malm aquifer with sour gas from a natural gas reservoir. Instead, the results indicate that the production of  $\text{H}_2\text{S}$  by TSR in the central basin is limited by the availability of methane and the rate of infiltrating sulfate from higher strata relative to the production rate. Both parameters will decrease during production when the system shifts from an equilibrium state to a kinetically controlled state. The decreasing salinity, gas loadings and  $\text{H}_2\text{S}$  concentrations during production support this conceptual model.

**Acknowledgements** Financial support by the Federal Ministry for the Environment, Nature Conservation and Nuclear Safety is gratefully acknowledged. We also would like to thank our project partners FU Berlin, Germany (coordinator), Erdwerk GmbH, Munich, Germany, and LfU Bayern, Munich, Germany for their support and D. Kirste for his very helpful suggestions during the review process.

## References

- Alawi M, Lerm S, Vetter A, Wolfgramm M, Seibt A, Würdemann H (2011) Diversity of sulfate reducing bacteria in a plant using deep geothermal energy. *Grundwasser* 16:105–112

- Andres G, Frisch H (1981) Hydrogeologie und Hydraulik im Malmkarst des Molassebeckens und der angrenzenden Fränkisch-Schwäbischen Alb [Hydrogeology and hydraulics in the Malm karst in the Molasse basin and the Swabian-Frankonian Alb]. *Schriftenr Bayer Landesamt Wasserwirtsch* 15:108–117
- Bailey AA, Smith JW (1972) Improved method for the preparation of sulfur dioxide from barium sulfate for isotope ratio studies. *Anal Chem* 44(8):1542–1543
- Baumann M, Quentin KE (1981) Hydrochemische Ergebnisse und Beurteilung des Thermal- und Schwefelwassers [Hydrochemical results and evaluation of the thermal and sulfuric waters]. *Schriftenr Bayer Landesamt Wasserwirtsch* 15:117–125
- Bayer Geol Landesamt (ed) (1996) Erläuterungen zur Geologischen Karte von Bayern 1:500000 [Explanation to the geological map of Bavaria 1:500000]. Bayer. Geol. Landesamt, Munich, Germany
- Berner RA (1980) Early diagenesis. Princeton University Press, Princeton, NJ
- Birner J, Mayr C, Thomas L, Schneider M, Baumann T, Winkler A (2011) Hydrochemie und Genese der tiefen Grundwässer des Malmaquifers im bayerischen Teil des süddeutschen Molassebeckens [Hydrochemistry and evolution of deep groundwaters in the Malm aquifer in the Bavarian part of the South German Molasse Basin]. *Z Geol Wiss* 39:291–308
- Carlé W (1975) Die Mineral- und Thermalwässer von Mitteleuropa [Mineral and thermal waters of Central Europe]. Wiss. Verlagsges., Stuttgart, Germany
- Clark ID, Fritz P (1997) Environmental isotopes in hydrogeology. CRC, New York
- Coleman ML, Shephard TJ, Durham JJ, Rouse JE, Moore GR (1982) Reduction of water with zinc for hydrogen isotope analysis. *Anal Chem* 54:993–995
- Craig H (1961) Isotopic variation in meteoric waters. *Science* 133:1702–1703
- Deutsches Institut für Normung (1995) DIN 51855–4: Prüfung von gasförmigen Brennstoffen und sonstigen Gasen - Bestimmung des Gehaltes an Schwefelverbindungen - Teil 4: Gehalt an Schwefelwasserstoff, Zinkacetat-Verfahren [Testing of gaseous fuels and other gases: determination of sulphur compounds content, part 4—content of hydrogen sulfide, zinc acetate method]. Beuth, Berlin
- Domenico PA, Schwartz W (1998) Physical and chemical hydrogeology. Wiley, New York
- Emery D, Robinson A (1993) Inorganic geochemistry: applications to petroleum geology. Blackwell, Oxford
- Epstein S, Mayeda T (1953) Variation of  $^{18}\text{O}$  content of waters from natural sources. *Geochim Cosmochim Acta* 4:213–224
- Friedman I (1953) Deuterium content of natural waters and other substances. *Geochim Cosmochim Acta* 4:89–103
- Goldbrunner JE (1997) Vergleich von Isotopenuntersuchungen an Tiefengrundwässern des Steirischen Beckens und des Oberösterreichischen Molassebeckens [Comparison of the isotopic data of deep groundwater in the Styrian Basin, Austria, and the Upper Austrian Molasse Basin]. *Mitt Österr Geol Ges* 88:31–39
- Goldhaber MB, Kaplan IR (1974) The sea. Wiley, Chichester, UK, pp 569–665
- Hesse R, Schmidt-Thomé P (1975) Neue Jodwasservorkommen im Bereich der bayerischen Alpenrand-Strukturen bei Bad Tölz [New iodine groundwater resources at the alpine structures near Bad Tölz, Bavaria, Germany]. *Geol Jahrb C* 11:31–66
- Jørgensen BB, Isaksen MF, Jannash HW (1992) Bacterial sulfate reduction above 100 °C in deep sea hydrothermal vent sediments. *Science* 258:703–704
- Krouse HR, Ritchie RGS, Roche RS (1987) Sulphur isotope composition of  $\text{H}_2\text{S}$  evolved during the non-isothermal pyrolysis of sulphur-containing materials. *J Anal Appl Pyrol* 12:19–29
- Krouse HR, Viau AA, Eliuk LS, Ueda A, Halas S (1988) Chemical and isotopic evidence of thermochemical sulphate reduction by light hydrocarbon gases in deep carbonate reservoirs. *Nature* 333:415–419
- Langmuir D (1971) Geochemistry of some carbonate ground waters in central Pennsylvania. *Geochim Cosmochim Acta* 35:1023–1045
- Lemcke K (1976) Übertiefe Grundwässer im süddeutschen Alpenvorland [Excess depth groundwater in Wouth Germany]. *Bull Ver Schweiz Petroleum-Geol Ing* 42:9–18
- Lemcke K (1988) Geologie von Bayern, I: Das bayerische Alpenvorland vor der Eiszeit [Geology of Bavaria, I: the Bavarian Alpine foothills before the Quaternary]. Schweizerbart, Stuttgart, Germany
- Liu QY, Worden RH, Jin ZJ, Liu WH, Li J, Gao B, Zhang DW, Hu AP, Yang C (2013) TSR versus non-TSR processes and their impact on gas geochemistry and carbon stable isotopes in Carboniferous, Permian and Lower Triassic marine carbonate gas reservoirs in the Eastern Sichuan Basin, China. *Geochim Cosmochim Acta* 100:96–115
- Macdonald DD, Roberts B, Hyne JB (1978) Corrosion of carbon steel during cyclical exposure to wet elemental sulphur and the atmosphere. *Corros Sci* 18(5):499–501
- Machel HG (1987) Some aspects of diagenetic sulphate-hydrocarbon redox-reactions. In: Marshall J (ed) Diagenesis of sedimentary sequences. *Geol Soc Spec Publ* 36, pp 15–28
- Machel HG (2001) Bacterial and thermochemical sulfate reduction in diagenetic settings: old and new insights. *Sediment Geol* 140:143–175
- Machel HG, Krouse HR, Sassen R (1995) Products and distinguishing criteria of bacterial and thermochemical sulfate reduction. *Appl Geochem* 10:373–389
- Morris DR, Sampaleanu LP, Veysey DN (1980) The corrosion of steel by aqueous-solutions of hydrogen-sulfide. *J Electrochem Soc* 127(6):1228–1235
- Nöth S (1997) High  $\text{H}_2\text{S}$  contents and other effects of thermochemical sulfate reduction in deeply buried carbonate reservoirs: a review. *Geol Rundsch* 86:275–287
- Orr WL (1974) Changes in sulfur content and isotope ratios of sulfur during petroleum maturation study of Big Horn basin Paleozoic oils. *AAPG Bull* 58(11):2295–2318
- Orr WL (1977) Geologic and geochemical controls on the distribution of hydrogen sulfide in natural gas. In: *Advances in Organic Geochemistry*. Enadisma, Madrid, pp 571–597
- Orr WL (1982) Rate and mechanism of non-microbial sulfate reduction. GSA, Boulder, CO, 580 pp
- Parkhurst DL, Appelo CAJ (1999) User's guide to PHREEQC (version 2): a computer program for speciation, batch-reaction, one-dimensional transport, and inverse geochemical calculations. US Geol Surv Water Resour Invest Rep 99–4259
- Perrin DD (1982) Ionization constants of inorganic acids and bases in aqueous solution. Pergamon, Oxford
- Prestel R, Stier P, Jobmann M, Schulz R, Straley G, Wendebourg J, Werner J, Wolf M, Eichinger L, Salvamoser J, Weise S, Fritz P (1991) Hydrogeothermische Energiebilanz und Grundwasserhaushalt des Malmkarstes im süddeutschen Molassebecken [Hydrogeothermal energy balance and groundwater balance of the Malm karst in the South German Molasse Basin]. Bayer. LfW und LGRB, Munich, Germany
- Reis MAM, Almeida JS, Lemos PC, Carrondo MJT (1992) Effect of hydrogen sulfide on growth of sulfate reducing bacteria. *Biotechnol Bioeng* 40:593–600
- Schulte U, Strauß H, Bergmann A, Obermann P (1997) Isotopenverhältnisse der Schwefel- und Kohlenstoffspezies aus Sedimenten und tiefen Grundwässern der Niederrheinischen Bucht [Isotopic ratios of sulfur and carbon species from sediments and deep groundwater in the lower Rhine Bay]. *Grundwasser* 2:103–110
- Stichler W, Rauert W, Weise S, Wolf M, Koschel G, Stier P, Prestel R, Hedin K (1987) Isotopenhydrologische und hydrochemische Untersuchungen zur Erkundung des Fließsystems im Malmkarstaquifer des süddeutschen Alpenvorlandes [Isotope hydrological and hydrochemical investigations of the flow

- regime in the Malm karst of the South German Alpine foothills]. *Z Dtsch Geol Ges* 138:387–398
- Tilley B, Baumann T (2012) On temperature attenuation in open-loop wells. *Renew Energy* 48:416–423
- Udluft P (1975) Das tiefere Grundwasser zwischen Vindelicischem Rücken und Alpenrand [The deep groundwater between Vindelician Crest and the Alps]. *Geol Jahrb C* 11:3–29
- Villinger E (1977) Über Potentialverteilung und Strömungssysteme im Karstwasser der Schwäbischen Alb [Hydraulic potential and flow regime of the groundwater in the karst of the Swabian Alb]. *Geol Jahrb C* 18:9–93
- Wagner B, Kus G, Kainzmaier B, Spörlein T, Wilferth T, Veit W, Fritsch P, Wrobel M, Lindenthal W, Neumann J, Sprenger W (2009) Erläuterungen zur Hydrogeologischen Karte von Bayern 1:500000 [Explanation to the hydrogeological map of Bavaria 1:500000]. Bayer. Landesamt f. Umwelt, Munich, Germany
- Wynn JG, Sumrall JB, Onac BP (2010) Sulfur isotopic composition and the source of dissolved sulfur species in thermo-mineral springs of the Cerna Valley, Romania. *Chem Geol* 271:31–43
- Zhu GY, Zhang SC, Liang YB (2007a) The controlling factors and distribution prediction of H<sub>2</sub>S formation in marine carbonate gas reservoir, China. *Chin Sci Bull* 52:150–163
- Zhu GY, Zhang SC, Liang YB, Li QR (2007b) The genesis of H<sub>2</sub>S in the Weiyuan Gas Field, Sichuan Basin and its evidence. *Chinese Sci Bull* 52(10):1394–1404